Integrated Analytical Strategies for Drug Discovery

de Vlieger, J.S.B.

2011

document version
Publisher's PDF, also known as Version of record

citation for published version (APA)
de Vlieger, J. S. B. (2011). *Integrated Analytical Strategies for Drug Discovery*.

Chapter 6

Development of an online p38α mitogen-activated protein kinase binding assay and integration of LC-HR-MS.

Abstract

A high resolution screening method was developed for the p38α mitogen-activated protein kinase to detect and identify small molecule binders. Its central role in inflammatory diseases makes this enzyme a very important drug target. The setup integrates separation by high performance liquid chromatography with two parallel detection techniques. High resolution-mass spectrometry gives structural information to identify small molecules while an online enzyme binding detection method provides data on p38α binding. The separation step allows the individual assessment of compounds in a mixture and links affinity and structure information via the retention time. Enzyme binding detection was achieved with a competitive binding assay based on fluorescence enhancement which has a simple principle, is inexpensive and easy to interpret. The concentrations of p38α and the fluorescence tracer SK&F86002 were optimized as well as incubation temperature, formic acid content of the LC eluents and the material of the incubation tubing. The latter notably improved the screening of highly lipophilic compounds. For optimization and validation purposes, the known kinase inhibitors BIRB796, TAK715 and MAPKI1 were used among others. The result is a high quality assay with Z'-factors around 0.8, which is suitable for semi-quantitative affinity measurements and applicable to various binding modes. Furthermore, the integrated approach gives affinity data on individual compounds instead of averaged ones for mixtures.

Introduction

Kinases are certainly among the most important target classes in contemporary drug discovery [1]. The mitogen-activated protein kinase p38 (p38) is one prominent example of a drug-target kinase especially its most important isoform p38α [2, 3]. It is involved in signal transduction pathways, transmitting signals through successive activation by phosphorylation [4]. Being one of the important mediators for a cell's response to extracellular stimuli, this pathway presents a promising opportunity for drug intervention [5]. Because p38α is heavily involved in inflammation processes, the envisaged diseases are mostly chronic inflammatory diseases like rheumatoid arthritis, psoriasis or Crohn's disease [6]. Several p38α inhibitors, which target these diseases, are currently in different

stages of preclinical and clinical development up to phase II [7, 3]. Nearly all known kinase inhibitors show interactions with the highly conserved ATP-binding pocket. Therefore, most early kinase inhibitors, possessing only these interactions, exhibited poor kinase selectivity [5]. Although different systems of categorization exist, these will be called type I inhibitors. Type I inhibitors used in this study are TAK715 [8], MAP kinase inhibitor 1 (MAPKI1) from Merck KGaA [9] and SK&F 86002 (SKF) [9]. The discovery of an allosteric binding pocket adjacent to the ATP-binding site led to the discovery of inhibitors using both sites (type II). BIRB796 is a prominent example of this type of binding [10, 11]. Consequently, type III binders like 1-(3-*tert*-butyl-1-methyl-1*H*-pyrazol-5-yl)-3-(4-chlorophenyl)urea (pyrazolourea) are targeting only this allosteric site [12]. The type IV inhibitors are not binding to either of the two pockets, as has been discovered e.g. for GNF-2 binding to the Brc-abl kinase [13]. The importance of p38α has led to a multitude of assay principles for the identification of small molecules targeting this kinase [14, 15]. Among the cell-free *in vitro* formats for p38α, those based on activity and those based on affinity can be distinguished. As readout for activity based methods, scintillation [11] and fluorescence polarization [16] have been used among others [14, 15]. These formats require expensive reagents (antibodies, etc.) and rely on labels which can impair the usefulness of results, or they involve handling radioactivity. In addition to these drawbacks, activity assays can, by definition, not employ the non-phosphorylated kinase as target. This is the advantage of affinity based assays. However, scintillation [17], chemiluminescence [16] and fluorescence polarization [18] suffer from similar reagent based drawbacks as mentioned above. Furthermore, some label free technologies, like surface plasmon resonance [16] or isothermal titration calorimetry [19], have been employed, which avoid additional reagents and the problems of molecular probes. Still, these techniques are complex and instrumental requirements and logistics may limit their throughput. A relatively simple approach was used by Pargellis *et al.* during the discovery of BIRB796 [10, 11]. The method is based on fluorescence enhancement and requires solely native p38 and the small molecule kinase inhibitor SKF. SKF shows fluorescence, which is strongly enhanced upon binding to the target enzyme. Therefore, high fluorescence intensity indicates a high concentration of the enzyme-tracer complex. A compound showing affinity to the target enzyme will compete with the tracer thus reducing the concentration of enzyme-tracer complex and thereby

reducing the fluorescence. This principle enables a competitive binding assay in a homogeneous setup, which is based on the strong difference in fluorescence intensity between the free tracer and the enzyme-tracer complex. Because of its convenience and the possibility to use non-phosphorylated p38α as target, this technique presented a good basis for the development of a high resolution screening (HRS) platform. HRS is defined by the combination of separation and screening in an integrated system. Therefore, it enables the affinity assessment and the simultaneous structural characterization of individual compounds in mixtures [20, 21]. This feature makes HRS platforms especially attractive when complex mixtures such as metabolic incubations [22], combinatorial mixtures [21] or natural extracts [23] are screened where dereplication, affinity and structural information are crucial. In contrast to conventional high throughput screening (HTS), isolation of individual compounds not showing affinity can be avoided. Thus, the laborious development of high yield synthesis and isolation methods can be limited to compounds showing the desired affinity. One common approach in HRS is the use of online post-column assays, which have been recently reviewed by Shi *et al.* [24]. Colourimetry, fluorescence and mass spectrometry based readouts were developed in both homogeneous and inhomogeneous formats. Homogeneous setups are easier to apply, so their significance exceeds inhomogeneous setups in cases where background fluorescence is of minor importance. However, HRS formats described so far are either activity based [21, 23] or target a receptor [20, 22]. We report the implementation of the enzyme p38α as the first kinase to be targeted in an online post-column binding assay (HRS system). Furthermore, the screening of highly lipophilic molecules was greatly improved by the unprecedented use of covalently modified fused silica tubing as material for post-column incubation, resulting in improved affinity signals.

Materials and Methods

Materials

Human recombinant p38α, ORG X, BIRB796 and TAK715 were a kind gift of MSD research laboratories (Oss, The Netherlands). SKF and MAPKI1 were purchased from Merck KGaA (Darmstadt, Germany). ELISA blocking reagent was delivered by Roche Diagnostics (Mannheim, Germany). Pyrazolourea was obtained from Ambinter (Paris, France). All other chemicals were from Sigma-Aldrich

(Schnelldorf, Germany). Fused silica tubing (250 μm inner and 375 μm outer diameter) untreated or covalently coated with PEG, methyl or methyl/phenyl groups was also purchased from Sigma-Aldrich (Schnelldorf, Germany). 96 'flat' bottom chimney well, black polypropylene microtiter plates from Greiner bio-one (Alphen a/d Rijn, The Netherlands) were used. Methanol (LC-MS Grade) and formic acid (ULC-MS Grade) were obtained from Biosolve (Valkenswaard, The Netherlands). Purified water was generated with a Milli-Q academic from Millipore (Amsterdam, The Netherlands).

Instrumentation

96 well plate experiments were performed on a Victor3 plate reader from Perkin-Elmer (Groningen, The Netherlands). The setup used for the online assay included two LC-20AD and two LC-10AD isocratic pumps, a SIL-20AC autosampler, one CTO-20AC and one CTO-10AC column oven, an RF-10AXL fluorescence detector, a CBM-20A controller and an Ion Trap-Time-of-flight (IT-TOF) mass spectrometer equipped with an ESI source all products of Shimadzu ('s Hertogenbosch, The Netherlands). HR-MS spectra were obtained from m/z 200 to 650 switching positive- and negative-ion mode with 10 ms accumulation time each. The curved desolvation line and the heating block were equilibrated at 200°C and the voltages applied were 5 kV to the interface and 1.7 kV to the detector. Nitrogen (99.9990%) was used at flows of 1.5 L/min and 10 L/min as nebulising gas and drying gas, respectively. To allow accurate mass measurements, external calibration of the IT-TOF was performed using TFA clusters. Furthermore, two superloops and two pulse dampeners made in house were used.

Plate Reader Assay

A 20 mM TRIS-HCl buffer (pH 7.5), containing 10 mM $MgCl_2$, 2 g/L PEG 6000 and 0.2 g/L ELISA blocking reagent (TRIS buffer), was used in all experiments. All solutions of p38α were prepared in TRIS buffer. Enzyme stock solutions were stored at -80°C until use. During online experiments, the enzyme solutions were kept at 0°C. A stock solution of SKF (2 mM) was made in DMSO and further diluted with TRIS buffer. Solutions of inhibitors were prepared in water:methanol 1:1 containing 0.01% formic acid from 2 mM or 5 mM stock solutions in methanol (DMSO in case of MAPKI1). Small molecules stock solutions were stored at -20°C.

For plate reader measurements, the wells were filled with 50 µL enzyme solution, 12.5 µL inhibitor solution and 50 µL SKF solution in the given order. Fluorescence was measured at 25°C with the wavelength of absorption and emission being 355±4 nm and 405±5 nm, respectively. The sum of ten flashes was used as readout to improve performance. Saturation of a 90 nM solution of p38α with SKF was determined by using a concentration range from 40 nM to 2500 nM of SKF. The Z'-factor is a measure for assay quality. If not otherwise stated, it was calculated according to the original publication of Zhang *et al.* [25]. A more detailed explanation is given in the results and discussion section. Measurements of the Z'-factor dependence on enzyme concentration were performed on three days with five repeats per day and a final concentration of 3 µM SKF. For full inhibition, TAK715 was added to a final concentration of 1 µM, while the control values contained only the corresponding amount (see above) of HPLC solvents.

Online Assay

HPLC solvents were water:methanol 100:1 (solvent A) and methanol:water 100:1 (solvent B) both containing 0.01% formic acid. The instrumental setup described by de Vlieger *et al.* [20] was used for the analysis with one enzyme binding detection line and the following modifications (cf Fig. 1). HPLC was done either in flow injection analysis mode (FIA – where no separation column is present) or with a SunFire C18 column 30 x 2.1 mm, 3.5 µm particles (Waters, Milford, MA, USA) (Fig. 1 - 2). 10 µL of the sample were injected (Fig. 1 - 1) into a flow of 113 µL/min. Elution was performed at 40°C either isocratic at different methanol concentrations or using a binary gradient. Post-column, the flow was split 1:9 (Fig. 1 - 3), sending 100 µL/min to high resolution/mass spectrometry (HR-MS) detection and 13 µL/min to the enzyme binding detection. To the 13 µL/min HPLC eluent, first 50 µL/min of a 200 nM p38α solution were added (Fig. 1 - 4) and thereafter 50 µL/min of a 1400 nM solution of SKF (Fig. 1 - 6). These solutions were constantly released by a linear setup of an LC-10AD pump, a pulse dampener with restriction capillary and a superloop each. Following each addition, the mixture was incubated in PEG deactivated fused silica loops of 25 µL (Fig. 1 - 5) and 20 µL (Fig. 1 - 7), respectively. The incubation loops were kept at 25°C in a second column oven. The resulting incubation times were 24 s for the target-ligand interaction (Fig. 1 - 5) and 11 s for the target-tracer interaction (Fig. 1 - 7). Finally, at concentrations of 90 nM p38α and 630 nM of SKF the

fluorescence was measured with excitation at 355±7.5 nm and emission at 425±7.5 nm (Fig. 1 - 8). The used detector settings were gain 4, recorder range 1 and sensitivity medium.
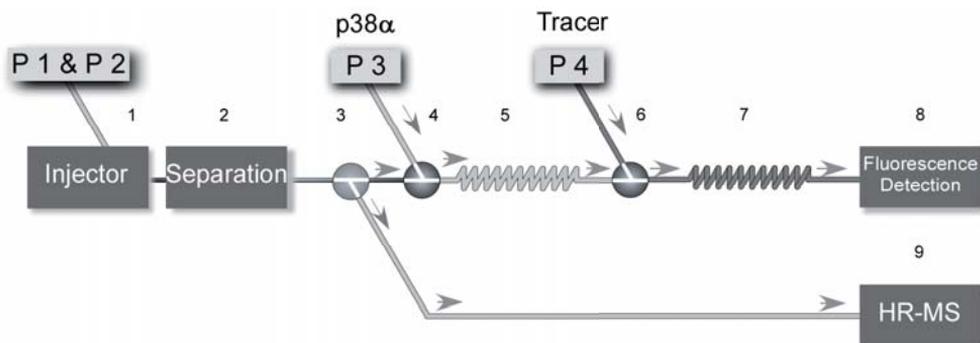

Figure 1. Scheme of the online setup. The system enables the separation of mixtures and subsequent parallel detection of enzyme binding and accurate mass. The samples are injected (1) into and separated (2) by an HPLC system. The eluent is split (3) between HR-MS and enzyme binding detection. The fraction which enters the enzyme binding detection is mixed with the target (4) and the tracer (6), and incubated after each mixing step, 24 s for the target-ligand interaction (5) and 11 s for the target-tracer interaction (7). Finally, the fluorescence is measured (8) as readout of affinity towards p38α. In parallel, the second part of the eluent is analyzed by HR-MS (9), delivering structural information to identify the small molecules tested.

The influence of the methanol concentration on the maximum signal was assessed in two consecutive measurements. To this end, a stepwise gradient was used starting at 100% A and increasing the fraction of B by 15% approximately every 10 min. In the first run, the baseline without inhibition was recorded. In the second run, MAPKI1 was added to the SKF solution for full inhibition, reaching a final assay concentration of around 0.9 µM. By comparing these measurements, the assay window in relation to the different organic modifier concentrations can be estimated.

In order to assess the influence of the incubation tubing material, two measurements were carried out, in which the volume and therefore the incubation time was kept constant: In the first experiment, polyether ether ketone (PEEK) of 250 µm and 170 µm inner diameter (ID), polytetrafluoroethylene (PTFE) of 250 µm ID and untreated fused silica of 250 µm ID were compared by injecting a 2 µM solution of ORG X in FIA mode at 60% B. In a second experiment, 250 µm ID fused silica tubing with covalent coatings of different polarity were compared. In these experiments, a 20 µM solution of ORG X was injected in FIA mode at 60% B. The coatings were PEG (polar), a mixture of phenyl and methyl groups (intermediate) or methyl groups only (non-polar).

The online Z'-factor was calculated from triplicate injections each of a control (blank) experiment and a full inhibition sample on five different days. The full inhibition sample was a mixture of 50 µM BIRB796, 20 µM ORG X and 20 µM TAK715 while the control sample was a 1:1 mixture of the solvents. The separation was carried out with the following gradient: 0 to 1.0 min isocratic at 50% B, 1.0 to 12.5 min linear to 90% B, 12.5 to 14.5 min isocratic at 90% B, 14.5 to 15.0 min linear to 50% B and 15.0 to 21.0 min isocratic at 50% B.

MAPKI1 and TAK715 were tested in a mixture with six drug molecules to simulate a screening situation. Carbamazepine, norethisterone, warfarin, phenylbutazone, celecoxib and diclofenac were used as test compounds without p38α affinity. TAK715 was injected at 20 µM concentration, the others at 50 µM. The mixture was separated with the following gradient: 0 to 2.0 min isocratic at 50% B, 2.0 to 32.0 min linear to 70% B, 32.0 to 38.0 min isocratic at 70% B, 38.0 to 38.5 min linear to 50% B and 38.5 to 50.0 min isocratic at 50% B.

For the measurements of IC_{50} values, isocratic elution was applied, taking care that the substance peak showed separation from the injection peak. TAK715 was eluted at 85% B, BIRB796 at 50% and MAPKI1 at 70%. Solutions of nine different concentrations for each inhibitor were prepared in 50% methanol, 50% water and 0.01% formic acid from 5 mM stock solutions of TAK715 and BIRB796 in methanol or a 2 mM stock solution of MAPKI1 in DMSO. The following concentrations for each inhibitor were prepared: 50 nM, 100 nM, 200 nM, 500 nM, 1 µM, 2 µM, 5 µM, 10 µM and 20 µM for TAK715; 500 nM, 1 µM, 2 µM, 5 µM, 10 µM, 20 µM 50 µM, 100 µM and 200 µM for BIRB796 and 200 nM, 500 nM, 1 µM, 2 µM, 5 µM,

10 µM, 20 µM 50 µM and 100 µM for MAPKI1. These nine concentrations and a blank were injected in triplicate for every inhibitor.

To finalise the binding mode studies, the pyrazolourea compound was used as an example of a type III inhibitor. It was injected at a concentration of 100 µM and tested under isocratic conditions at 70% B.

Results and Discussion:

Assay conditions optimization

Optimization was carried out in a 96 well format. The protocol of Regan *et al.* [10] was used with some modifications. Since Mg^{2+} ions are known to be involved in ATP binding and can potentially influence binding of inhibitors to the ATP binding site, $MgCl_2$ was added. Furthermore, ELISA blocking reagent and PEG 6000 were added in order to avoid non-specific binding and unwanted interactions with the material of the enzyme binding detection [26]. Enzyme and tracer concentrations were optimized under these conditions. The fluorescence signal showed a linear dependence on the enzyme concentration (cf Online Resource 1 Fig. S1). The most suitable p38α concentration was therefore chosen considering the Z'-factor measurements. The signal dependence on the tracer concentration, depicted in Fig. 2A, displays the asymptotic form of saturation behaviour. The final concentration of 630 nM SKF is selected to be slightly above the saturation value. This choice presents a compromise between avoiding deviations of the signal due to variability in the tracer concentration and maximising the sensitivity with regard to detection limits for binders. Namely, competition reduces this sensitivity with increasing tracer concentration.

There are several factors mainly related to the HPLC separation system, which can have a negative influence on the assay performance. Methanol, formic acid and the incubation temperature are the most prominent of these variables. Using typical HPLC conditions such as 50% methanol and 0.1% formic acid at 37°C completely inhibited the fluorescence enhancement. As a result, these factors were carefully optimized and need to be controlled cautiously. The influence of organic modifier at no and full inhibition is shown in Fig. 2B. The assay window decreased with increasing organic modifier (methanol) content. However, the Z'_{chrom}-factors for the different compounds measured at different MeOH

147

concentrations, due to gradient elution, showed only minor differences thereby proving the robustness of the online setup even at high methanol concentrations. Increasing temperature also yielded a similar decrease in maximum signal as seen with methanol. In order to guarantee robustness and enable the use of up to 90% methanol in the HPLC separation, the formic acid concentration in the eluent and the incubation temperature were restricted to 0.01% and 25°C, respectively. Hence, the temperatures of the HPLC separation step and the enzyme binding detection were controlled separately.
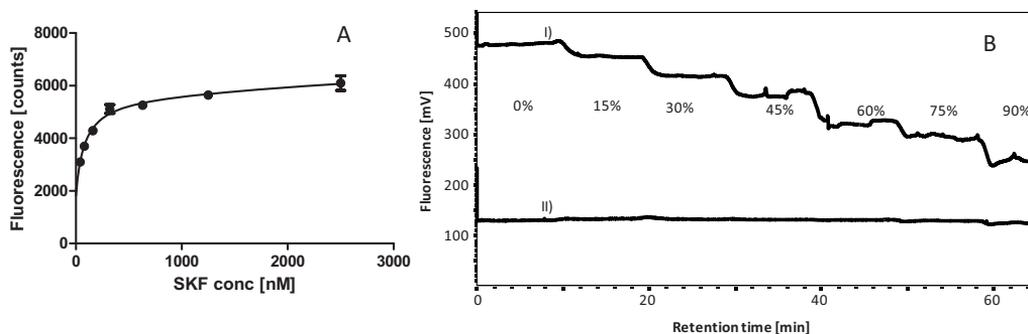

Figure 2. Optimization of the p38α affinity assay.

A) Saturation curve of the tracer for 90 nM p38α (n=3). Full saturation was reached at 630 nM SKF, which was consequently the selected tracer concentration.

B) Influence of the organic modifier concentration on the enzyme binding detection. I) is the baseline at different percentages of organic modifier in HPLC mobile phase, which shows the maximum signal reached at these different MeOH concentrations. In opposition, line II) shows the fluorescence signal at maximum inhibition hence the difference between both lines describes the maximum assay window. II) was measured by premixing SKF with MAPKI1 (900 nM final concentration) in the superloop.

The screening of highly lipophilic compounds is not only challenging in offline screening due to adhesion and solubility issues [27] but also presents challenges in online screening approaches [26]. In online screening systems, the amount of organic modifier is usually kept low to prevent protein degradation. On the other hand, the tubing used for incubation loops is mostly PEEK or PTFE. The favoured interaction of non-polar compounds with these surfaces results in peak
148

broadening and tailing, thus decreasing resolution and sensitivity. By using polar material for the incubation loops, this effect was significantly decreased. Fig. 3A shows a two to threefold increase in signal height and reduced tailing when untreated fused silica tubing is used instead of PEEK. Although, PTFE compared to PEEK already yields decreased peak width, the width is additionally approximately halved with untreated fused silica. The polarity of the incubation coil material plays a crucial role explaining these findings. This can clearly be seen in Fig. 3B where the influence of fused silica tubing with covalent coatings of different polarities on the peak shape was compared. The polar (PEG coated) tubing gave the best results while peak height and shape degraded towards intermediate (methyl/phenyl coated) and non-polar (methyl coated) surfaces. This indicates the influence of tubing polarity on post-column band broadening and justifies a preference of polar coated fused silica tubing over PEEK and PTFE in the presented study, taking the structural features of the studied compounds into account.
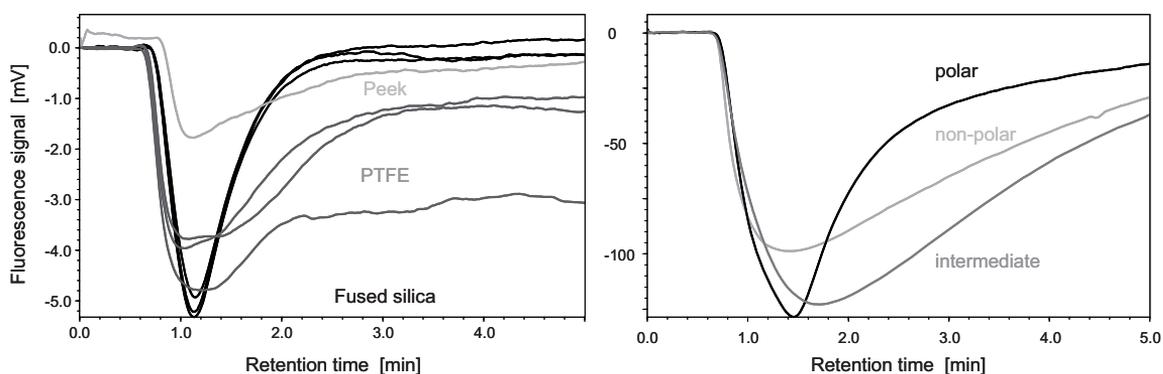

Figure 3. Influence of the reaction coil material on the peak shape. **A)** PEEK and PTFE were compared with untreated fused silica tubing. A 2 µM solution of ORGX was injected in FIA mode at 60% methanol. **B)** At the same conditions, a 20 µM solution of the same inhibitor was injected. Fused silica tubing with covalent coatings of either PEG (polar), a mixture of methyl and phenyl groups (intermediate) or only methyl groups (non-polar) was compared for their influence. In both experiments, peak width and asymmetry increased with decreasing polarity while the peak height decreased as a consequence. Fused silica tubing, coated with PEG (polar), exhibited drastically improved performance over the compared materials

Validation of the p38α binding assay

The quality of the p38α binding assay was assessed using the method of Zhang *et al.* [25]. The Z'-factor is introduced as a single value to judge assay quality, because it incorporates the SD of signal and background as well as the assay window. Therefore, it indicates the ability to distinguish between signals and false positives or false negatives. According to this method, the Z'-factor was calculated with equation 1 for several enzyme concentrations in the plate reader based setup. μ_s and μ_c are defined as the average signal of the sample and the control, respectively. Consequently, σ_s and σ_c are the standard deviations (SD) of these values.

$$Z' = 1 - \frac{(3\sigma_s + 3\sigma_c)}{|\mu_s - \mu_c|}$$

(1)

For the sake of comparability, the number of experiments (n=15) was kept the same in plate reader and online based measurements. However, this is recognized as a relatively low number for plate reader experiments. Therefore, an additional plate reader experiment with n=50 was performed, yielding a Z'-factor of -0.02. The conclusion from both experiments was as follows: The plate reader based assay at 90 nM p38α gave insufficient results with Z'-factors lower than 0. In the plate reader assay, a Z'-factor above 0.5, indicating an excellent assay, could only be achieved by raising the p38α concentration to 450 nM. Table 1 compares this data with the results of the online setup, in which 90 nM p38α was sufficient for an excellent assay. As a confirmation, the signal to noise ratios (S/N) were also calculated (Table 1), resulting in the same conclusions.

Table 1: Z'-factors and signal to noise rations (S/N) for plate reader and/or online based enzyme binding detection

	Inhibitor [a]	c (p38α) [nM]	Z' or Z'$_{chrom}$ [b] (n=15)	S/N
Plate reader	TAK715	90	-0.41	4
		180	0.49	12
		270	0.36	23
		360	0.49	55
		450	0.75	48
Online	BIRB796	90	0.77	70
	ORGX	90	0.82	106
	TAK715	90	0.80	97

[a] Concentration of the inhibitor was 1 µM TAK715 (final concentration) in the plate reader experiments. In the online setup ORG X and TAK715 were injected at 20 µM concentration and BIRB796 at 50 µM concentration for this purpose.

[b] In the plate reader experiments the Z'-factor was calculated according to equation 1. For the online experiments, equation 2 was used, yielding the Z'$_{chrom}$-factor.

Regardless of the findings of the last paragraph, the online setup has two disadvantages. Reagent consumption is usually higher in an online setup than in a plate reader based assay. Furthermore, the separation step introduces an additional dilution due to chromatographic peak broadening, which requires higher analyte concentrations. There are additional differences between the two setups, which should be adequately reflected in the Z'-factor. Kool *et al.* already applied the Z'-factor to chromatography based online assays, adapting the variables of equation 1 in order to take into account these discrepancies [28]. A main advantage is the internal control value (μ_c) represented by the baseline, which is more relevant than an external control, because it is available for each individual experiment. For a complete consideration of the differences between the online and the plate reader setup, all classical variables are systematically substituted with parameters more suitable to the online approach. Doing this without compromising the comparability of this Z'-factor is not trivial but possible. The assay window (μ_c-μ_s), as determined by the difference of the mean of control

151

(no inhibition) and signal (full inhibition), could more suitably be expressed as the mean of the peak height of full inhibition (μ_H), thereby still describing the desired parameter. Thus, the assay window is automatically corrected for changes in the baseline, representing the internal control. The SD of the sample (σ_s) would then consequentially be identified with the SD of the peak heights at full inhibition. For the control, usually no signals are obtained and changes of the baseline between samples are irrelevant as they have already been taken into account. The SD of the control (σ_c) can therefore logically be identified with the baseline deviation within one sample. This value is in chromatography better known as the noise. The measure of three times the noise is often used as limit of detection. This is consistent with the ideas behind the Z'-factor as both interpretations of $3\sigma_c$ are aimed at avoiding false positives. In summary, the transition from an external control to an internal one strengthens the reproducibility and accuracy of the assay and should therefore be appropriately reflected in the determination of Z'-factors. Therefore, an adjusted Z'-factor for the use in online systems is proposed in equation 2 on basis of the previous argumentation.

$$Z'_{chrom} = 1 - \frac{\left(3SD_H + 3 \cdot noise\right)}{\left|\mu_H\right|}$$

(2)

The new interpretation of the Z'-factor could also be used to omit the measurements of a control, significantly shortening the time of Z'$_{chrom}$-factor determination. Because the noise is calculated from the baseline of the chromatogram, a prerequisite is to have an empty time frame to observe both required values. Therefore, the first 4 min of the enzyme binding detection chromatogram were used to determine the noise. The mean noises calculated from signal and control runs were identical, thus proving the redundancy of the control measurements for Z'$_{chrom}$-factor determinations.
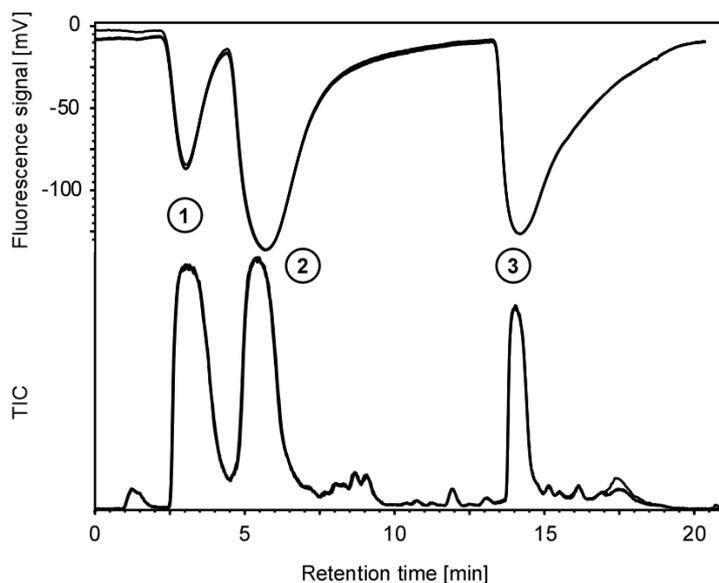
Figure 4. Comparison of MS and enzyme binding detection chromatogram. The matching of the fluorescence trace of the enzyme binding detection (above) and the total ion current (TIC) of the MS (below) for BIRB796 (1), ORGX (2) and TAK715 (3) are shown. Depicted is a triplicate from the Z'_{chrom}-factor determination. The excellent reproducibility in response, peak shape and retention time are clearly visible for both the enzyme binding detection and the MS signal. The low variability enables an easy and accurate matching of the two traces.

The repeatability of triplicates is excellent, which is clearly visible in Fig. 4, 5 and 6. This is true for the enzyme binding detection responses as well as for the chromatographic parameters like peak width, measured as full width at half maximum (FWHM), and retention time (t_r). For the enzyme binding detection, the relative SDs are ≤10% for FWHM and <3% for t_r. Low variability and noise compared to the total signal results in the high Z'-factor and signal-to-noise ratio (S/N) shown in table 1. The high Z'-factors indicate the excellent intra- and interday reproducibility, However, the online setup showed comparable Z'-factors at five times lower enzyme concentration than needed in the plate based assay. This is directly related to the minimal measurable IC_{50}. While IC_{50} values down to 45 nM can be distinguished in the online method, the plate reader method only

allows differentiation of IC_{50} values of 230 nM and higher. Furthermore, the higher enzyme concentration needed diminishes the advantage of the plate setup with regard to reagent consumption. Therefore, the online setup has advantages beside the additional possibilities associated with separation.

High resolution screening of mixtures

In order to assess whether the presented HRS method was suitable for the identification of small molecule binders of p38α in mixtures, a solution of eight compounds was screened. Two of these were the kinase inhibitors MAPKI1 and TAK715 while the other six were drug molecules from different classes. As illustrated in Fig. 5, all eight compounds could be separated for individual identification and affinity assessment. Based on HR-MS data, the structure was linked to a retention time. Accurate mass measurements enabled the unambiguous distinction of all compounds as two of them differed by less than 0.05 u. In case of more scarce knowledge of the sample, structure elucidation can be facilitated by HR-MS^n experiments [21]. In parallel to the structure confirmation, the retention time is also linked with affinity information through the enzyme binding detection. However, the readout of the enzyme binding detection is delayed compared to the HR-MS readout, because of a higher void volume and a lower average flow rate after splitting. This delay was measured to be 0.5 min by comparing both detection times in several experiments. It remains constant as long as void volume and flow rates are unchanged. The retention time corrected for this delay is used to couple affinity to identity information. Two affinity peaks were detected, which were linked to the elution of the kinase inhibitors. In conclusion, the approach presents a fast method to match the structure and activity of compounds in mixtures.
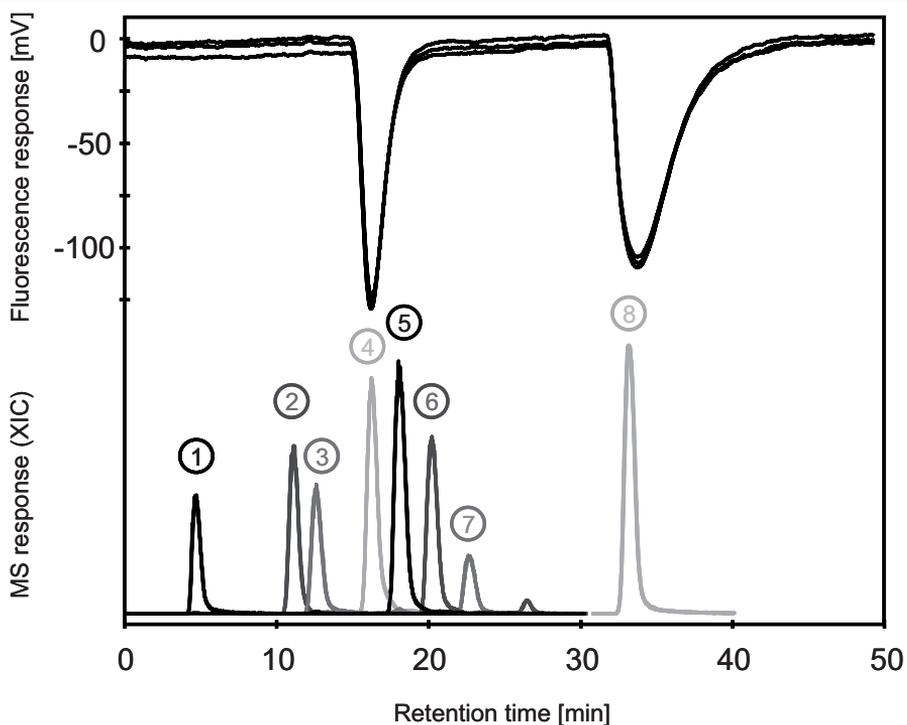
Figure 5. HRS of a mixture of kinase inhibitors and drug molecules. MAPKI1 (4) and TAK715 (8) were mixed with carbamazepine (1), norethisterone (2), warfarin (3), phenylbutazone (5), celecoxib (6) and diclofenac (7). The mixture was separated by HPLC and measured with HR-MS and enzyme binding detection in parallel. Accurate mass measurements with low deviation (<8ppm) and well matching isotope patterns allowed unambiguous identification. Structure and affinity were easily matched via the corrected retention times. Consequently, the two affinity compounds were detected in the mixture

Semi-Quantitative affinity measurements

Several known p38α inhibitors were tested for their dose related responses in the enzyme binding detection. Therefore, their injected concentrations had to be converted to final assay concentrations by taking into account the dilution factors. On one hand, splitting of the HPLC eluent and subsequent mixing with the reagents leads to dilution. This can be easily calculated from the ratios of the flow

in the beginning and the end of the enzyme binding detection (113/13 = 9). On the other hand, the chromatographic dilution, meaning the transition from an injected plug to a series of peaks of (assumed) Gaussian shape, has to be taken into account. The corresponding calculations have been described elsewhere [29]. The necessary peak parameters were taken from the enzyme binding detection. By dividing the injected concentration by the product of both dilution factors, the final concentration at maximum peak height can be calculated and used in the IC_{50} calculations (for a brief description see Online Resource 1).

Dose-response curves depicted in Fig. 6 were measured in triplicate with excellent R^2-values of >0.998 and minimal standard deviation (SD) of the triplicates (<2% SD relative to assay window). This shows again the excellent reproducibility and accuracy of the assay. The IC_{50} values and, given in brackets, their 95% confidence intervals, calculated after correcting the concentrations for the dilution factors are 81 nM (71 to 92 nM) for TAK715, 400 nM (360 to 440 nM) for BIRB796 and 760 nM (530 to 1100 nM) for MAPKI1. If the inhibitors are ranked for their affinity, the obtained results are in agreement with other methods, stating values of 7.1 nM for TAK715 [8], 18 nM for BIRB796 [10] and 35 nM for MAPKI1 [9]. However, the absolute values of measurements are 10 to 20 times higher than in literature. This can be explained by the profound differences in the assay formats. While the reported method gives affinities, the reference values were obtained by either activity assays (TAK715) or cell based functional assays (BIRB796, MAPKI1). Another specific reason responsible for this deviation is the slow binding kinetics of BIRB796. This compound is known to show an up to 12-fold deviation of its IC_{50} value, depending on the incubation time [11]. Despite the aforementioned issues, the method was proven to be suitable for the semi-quantitative assessment of small molecule relative affinities towards p38α serving as a selection tool in the drug discovery process.
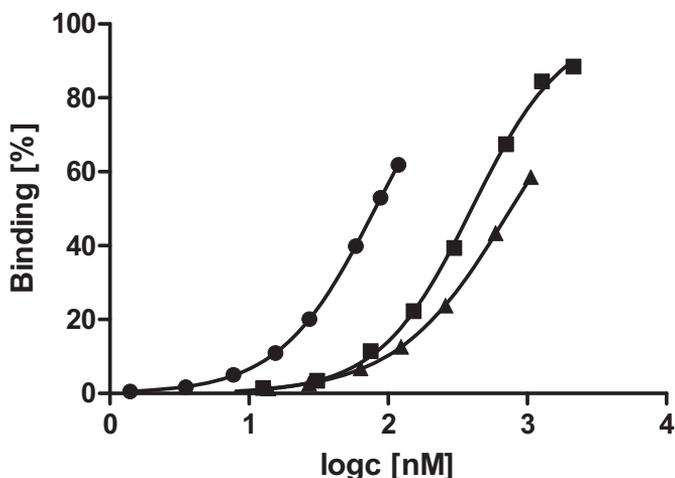
Figure 6. Semi-quanitative data of the tested p38α inhibitors. Binding curves are depicted for several known p38α inhibitors. The inhibitors TAK715 (circles), BIRB796 (squares) and MAPKI1 (triangles) are shown. Standard deviations of triplicate measurements were smaller than data point size

Applicability and binding modes

The type of binding to p38α as discussed in the introduction can have a significant influence on the ability of a screening technology to detect this binding. SKF is a type I binder and should therefore enable the detection of type I and type II binders as they compete for the ATP-binding pocket. This has been proven by the detection of TAK715 and MAPKI1 (type I) as well as BIRB796 (type II). Furthermore, structural changes in p38α upon binding of type III inhibitors may allow the detection of such compounds. The rearrangement of p38α from the DFG-in to the DFG-out conformation results in a reorientation of Phe405 thereby affecting the ATP-binding pocket. Hence, we tested the pyrazolourea structure, which was discussed by Simard *et al.* as an example of a type III inhibitor [12]. Fig. 7 shows the enzyme binding detection of this compound to p38α, thereby proving the suitability of the method for the detection of type III inhibitors. Consequently, the assay is capable of detecting a wide range of p38α binders including type I, II and III binders.
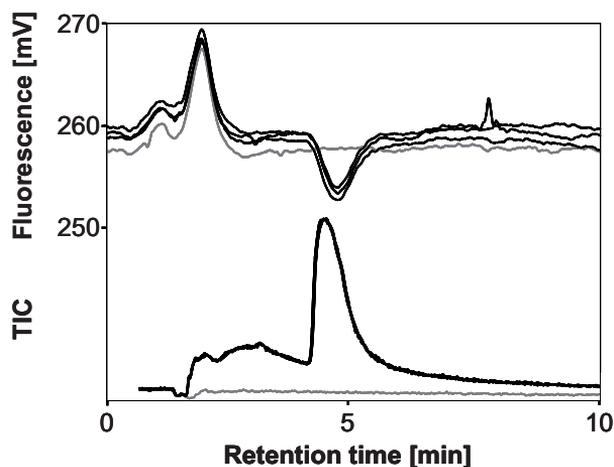
Figure 7. Detection of the binding of the pyrazolourea type III inhibitor to p38α. Triplicate injections of the inhibitor (black) showed signals in the enzyme binding detection (top). In contrast, the control (grey) did not show binding to p38α. HR-MS (bottom) confirmed the pyrazolourea compound as the binder. This clearly shows the ability of the assay to detect type III inhibitors. In combination with Fig. 4 it proves the applicability to several types of p38α inhibitors (types I, II and III).

Conclusion

An online binding assay for the separation and parallel assessment of identity and affinity of small molecules in complex mixtures towards non-phosphorylated p38α was developed. In terms of applicability, the scope of the presented HRS platform is different from conventional HTS assays. HTS is more suited for the screening of huge libraries where speed and low sample consumption are essential. The value of HRS lies in the parallel determination of structural and biochemical data of potential binders. While an HTS assay will only give a sum of compound affinities, HRS gives individual information on all (separated) molecules. The aim was to make available the advantages of the online approach, mainly the measurement of mixtures and a comparison of structure and affinity, for the important drug target p38α. An online post-column enzyme binding detection based on fluorescence enhancement was developed and its compatibility with modern HPLC separation techniques, such as gradient elution and increased temperature,

was demonstrated. HR-MS as parallel readout is an integral part of the developed screening platform, allowing the identification of the tested molecules. Additionally, the prospects of measuring compounds individually in mixtures were demonstrated by matching identity and affinity. Regarding the presented assay validation data, it can be stated that a high quality assay was achieved. Finally, the assay provided ranking of various p38α inhibitors (types I, II and III) allowing the use within a drug discovery process.

Acknowledgements

References

1. Cohen P (2002) Protein kinases-the major drug targets of the twenty-first century? Nat Rev Drug Discov 1 (4):309-315

2. Zhang J, Shen B, Lin A (2007) Novel strategies for inhibition of the p38 mapk pathway. Trends Pharmacol Sci 28 (6):286-295

3. Kumar S, Boehm J, Lee JC (2003) P38 map kinases: Key signalling molecules as therapeutic targets for inflammatory diseases. Nat Rev Drug Discov 2 (9):717-726

4. Saklatvala J (2004) The p38 map kinase pathway as a therapeutic target in inflammatory disease. Curr Opin Pharmacol 4 (4):372-377

5. Schindler JF, Monahan JB, Smith WG (2007) P38 pathway kinases as anti-inflammatory drug targets. J Dent Res 86 (9):800-811

6. Mayer RJ, Callahan JF (2006) P38 map kinase inhibitors: A future therapy for inflammatory diseases. Drug Discov Today 3 (1):49-54

7. Goldstein DM, Kuglstatter A, Lou Y, Soth MJ (2010) Selective p38alpha inhibitors clinically evaluated for the treatment of chronic inflammatory disorders. J Med Chem 53 (6):2345-2353

8. Miwatashi S, Arikawa Y, Kotani E, Miyamoto M, Naruo K, Kimura H, Tanaka T, Asahi S, Ohkawa S (2005) Novel inhibitor of p38 map kinase as an anti-tnf-alpha drug: Discovery of n-[4-[2-ethyl-4-(3-methylphenyl)-1,3-thiazol-5-yl]-2-pyridyl]benzamide (tak-715) as a potent and orally active anti-rheumatoid arthritis agent. J Med Chem 48 (19):5966-5979

9. de Laszlo SE, Visco D, Agarwal L, Chang L, Chin J, Croft G, Forsyth A, Fletcher D, Frantz B, Hacker C, Hanlon W, Harper C, Kostura M, Li B, Luell S, MacCoss M, Mantlo N, O'Neill EA, Orevillo C, Pang M, Parsons J, Rolando A, Sahly Y, Sidler K, O'Keefe SJ (1998) Pyrroles and other heterocycles as inhibitors of p38 kinase. Bioorg Med Chem Lett 8 (19):2689-2694

10. Regan J, Breitfelder S, Cirillo P, Gilmore T, Graham AG, Hickey E, Klaus B, Madwed J, Moriak M, Moss N, Pargellis C, Pav S, Proto A, Swinamer A, Tong L, Torcellini C (2002) Pyrazole urea-based inhibitors of p38 map kinase: From lead compound to clinical candidate. J Med Chem 45 (14):2994-3008

11. Pargellis C, Tong L, Churchill L, Cirillo PF, Gilmore T, Graham AG, Grob PM, Hickey ER, Moss N, Pav S, Regan J (2002) Inhibition of p38 map kinase by utilizing a novel allosteric binding site. Nat Struct Biol 9 (4):268-272

12. Simard JR, Klüter S, Grütter C, Getlik M, Rabiller M, Rode HB, Rauh D (2009) A new screening assay for allosteric inhibitors of csrc. Nat Chem Biol 5 (6):394-396

13. Adrian FJ, Ding Q, Sim T, Velentza A, Sloan C, Liu Y, Zhang G, Hur W, Ding S, Manley P, Mestan J, Fabbro D, Gray NS (2006) Allosteric inhibitors of bcr-abl-dependent cell proliferation. Nat Chem Biol 2 (2):95-102

14. Klumpp M, Boettcher A, Becker D, Meder G, Blank J, Leder L, Forstner M, Ottl J, Mayr LM (2006) Readout technologies for highly miniaturized kinase assays applicable to high-throughput screening in a 1536-well format. J Biomol Screen 11 (6):617-633

15. Olive DM (2004) Quantitative methods for the analysis of protein phosphorylation in drug development. Expert Rev Proteomics 1 (3):327-341

16. Zaman GJ, van der Lee MM, Kok JJ, Nelissen RL, Loomans EE (2006) Enzyme fragment complementation binding assay for p38alpha mitogen-activated protein kinase to study the binding kinetics of enzyme inhibitors. Assay Drug Dev Technol 4 (4):411-420

17. Lee JC, Laydon JT, McDonnell PC, Gallagher TF, Kumar S, Green D, McNulty D, Blumenthal MJ, Heys JR, Landvatter SW, Strickler JE, McLaughlin MM, Siemens IR, Fisher SM, Livi GP, White JR, Adams JL, Young PR (1994) A protein kinase involved in the regulation of inflammatory cytokine biosynthesis. Nature 372 (6508):739-746

18. Munoz L, Selig R, Yeung YT, Peifer C, Hauser D, Laufer S (2010) Fluorescence polarization binding assay to develop inhibitors of inactive p38alpha mitogen-activated protein kinase. Anal Biochem 401 (1):125-133

19. Young PR, McLaughlin MM, Kumar S, Kassis S, Doyle ML, McNulty D, Gallagher TF, Fisher S, McDonnell PC, Carr SA, Huddleston MJ, Seibel G, Porter TG, Livi GP, Adams JL, Lee JC (1997) Pyridinyl imidazole inhibitors of p38 mitogen-activated protein kinase bind in the atp site. J Biol Chem 272 (18):12116-12121

20. de Vlieger JS, Kolkman AJ, Ampt KA, Commandeur JN, Vermeulen NP, Kool J, Wijmenga SS, Niessen WM, Irth H, Honing M (2010) Determination and identification of estrogenic compounds generated with biosynthetic enzymes using hyphenated screening assays, high resolution mass spectrometry and off-line nmr. J Chromatogr B 878 (7-8):667-674

21. Giera M, de Vlieger JS, Lingeman H, Irth H, Niessen WM (2010) Structural elucidation of biologically active neomycin n-octyl derivatives in a regioisomeric mixture by means of liquid chromatography/ion trap time-of-flight mass spectrometry. Rapid Commun Mass Spectrom 24 (10):1439-1446

22. Van Liempd SM, Kool J, Meerman JH, Irth H, Vermeulen NP (2007) Metabolic profiling of endocrine-disrupting compounds by on-line cytochrome p450 bioreaction coupled to on-line receptor affinity screening. Chem Res Toxicol 20 (12):1825-1832

23. Giera M, Heus F, Janssen L, Kool J, Lingeman H, Irth H (2009) Microfractionation revisited: A 1536 well high resolution screening assay. Anal Chem 81 (13):5460-5466

24. Shi SY, Zhou HH, Zhang YP, Jiang XY, Chen XQ, Huang KL (2009) Coupling hplc to on-line, post-column (bio)chemical assays for high-resolution screening of bioactive compounds from complex mixtures. Trac-Trends in Analytical Chemistry 28 (7):865-877

25. Zhang JH, Chung TD, Oldenburg KR (1999) A simple statistical parameter for use in evaluation and validation of high throughput screening assays. J Biomol Screen 4 (2):67-73

26. Kool J, van Liempd SM, Ramautar R, Schenk T, Meerman JH, Irth H, Commandeur JN, Vermeulen NP (2005) Development of a novel cytochrome p450 bioaffinity detection system coupled online to gradient reversed-phase high-performance liquid chromatography. J Biomol Screen 10 (5):427-436

27. Schebb NH, Falck D, Faber H, Hein EM, Karst U, Hayen H (2009) Fast method for monitoring phospholipase a2 activity by liquid chromatography-electrospray ionization mass spectrometry. J Chromatogr A 1216 (27):5249-5255

28. Kool J, van Marle A, Hulscher S, Selman M, van Iperen DJ, van Altena K, Gillard M, Bakker RA, Irth H, Leurs R, Vermeulen NP (2007) A flow-through fluorescence polarization detection system for measuring gpcr-mediated modulation of camp production. J Biomol Screen 12 (8):1074-1083

29. Schebb NH, Heus F, Saenger T, Karst U, Irth H, Kool J (2008) Development of a countergradient parking system for gradient liquid chromatography with online biochemical detection of serine protease inhibitors. Anal Chem 80 (17):6764-6772